GEOPHYSICS, VOL. 81, NO. 1 (JANUARY-FEBRUARY 2016); P. V7–V16, 7 FIGS.
10.1190/GEO2015-0069.1

A fast algorithm for sparse multichannel blind deconvolution

Kenji Nose-Filho[1], André K. Takahata[2], Renato Lopes[1], and João M. T. Romano[1]

ABSTRACT

We have addressed blind deconvolution in a multichannel framework. Recently, a robust solution to this problem based on a Bayesian approach called sparse multichannel blind deconvolution (SMBD) was proposed in the literature with interesting results. However, its computational complexity can be high. We have proposed a fast algorithm based on the minimum entropy deconvolution, which is considerably less expensive. We designed the deconvolution filter to minimize a normalized version of the hybrid l_1/l_2-norm loss function. This is in contrast to the SMBD, in which the hybrid l_1/l_2-norm function is used as a regularization term to directly determine the deconvolved signal. Results with synthetic data determined that the performance of the obtained deconvolution filter was similar to the one obtained in a supervised framework. Similar results were also obtained in a real marine data set for both techniques.

INTRODUCTION

One important goal of seismic signal processing is to determine the subsurface reflectivity function, which is information of great interest for several applications, including oil exploration (Robinson, 1954; Porsani and Ursin, 1998; Yilmaz, 2001; Misra and Chopra, 2011). However, the seismic traces are actually a blurred version of the reflectivity. This blurring is caused by the fact that the seismic wavelet is not an ideal impulse, having instead a finite, nonzero duration. In fact, the seismic data can be modeled as the convolution of the reflectivity function and the seismic wavelet. To remove the effects of the wavelet from the data, and thus recover the reflectivity, we use a process called deconvolution.

Deconvolution has a very long and rich history in seismic processing and beyond (Kundur and Hatzinakos, 1996; Proakis, 2001). One particular challenge in the seismic case is that, in general, neither the reflectivity nor the wavelet can be assumed to be known. (In contrast, in communication systems, data are transmitted in blocks that begin with a known signal. This is used to determine the deconvolution systems, which are then used to deconvolve the actual, unknown, data in the remainder of the block.) Thus, one must resort to a body of techniques known as blind deconvolution (Romano et al., 2011). For a thorough account of the several kinds of blind deconvolution methods that have been applied in seismic signal processing, we refer the reader to the "Introduction" section in Kazemi and Sacchi (2014).

Of particular interest to this paper are the so-called multichannel blind deconvolution methods (Wiggins, 1978; Xu et al., 1995; Inouye and Sato, 1996; Rietsch, 1997a, 1997b; Kaaresen and Taxt, 1998; Ding and Li, 2001; Ram et al., 2010). The term multichannel comes from the fact that these methods are applied when we have several observations of a certain signal, and each observation goes through a different channel. This is exactly the case with seismic data, in which the same wavelet affects all traces, and the different channels are the different reflectivities in each trace. One of the very interesting properties of multichannel methods is that they yield an exact, algebraic estimation of the reflectivity in the noiseless case.

However, multichannel methods cannot be applied directly in the seismic case. Among other reasons, this happens because of the large similarity between neighboring reflectivities, which makes the problem either numerically unstable or, at worst, ill posed and impossible to solve. To overcome this problem, Kazemi and Sacchi (2014) propose a Bayesian approach in which the hybrid l_1/l_2-norm loss function is used as a sparsity-promoting regularization function. This technique, called sparse multichannel blind deconvolution (SMBD), presents good results in the synthetic and real data scenarios. However, it has a high computational cost.

In this paper, we propose a faster algorithm for SMBD based on the minimum entropy deconvolution (MED) algorithm. MED is another sparsity-promoting blind deconvolution approach, widely explored during the 1980s (Claerbout, 1977; Gray, 1978b; Wiggins,

Manuscript received by the Editor 2 February 2015; revised manuscript received 1 September 2015; published online 16 November 2015.
[1]University of Campinas, School of Electrical and Computer Engineering, Campinas, Brazil. E-mail: knfilho@dmo.fee.unicamp.br; rlopes@decom.fee.unicamp.br; romano@decom.fee.unicamp.br.
[2]University of Campinas, School of Electrical and Computer Engineering and DSPGeo, Campinas, Brazil. E-mail: andre@dspgeo.com.

1978; Ooe and Ulrych, 1979; Donoho, 1981; Cabrelli, 1985). In this case, a sparse signal is defined as a signal composed of a few spikes, of unknown amplitude and position, separated by nearly zero terms (Wiggins, 1978). (The parallel between sparsity and entropy drawn by Wiggins [1978] is that sparse signals, being well-organized, should have a small entropy.) By observing that the convolution of such a signal with the seismic wavelet would lead to a less sparse signal, Wiggins (1978) proposed a technique based on linear filtering that searches for the filter that leads to the most sparse output, which would correspond to the estimated reflectivity.

In summary, the main idea of MED algorithms is to estimate a deconvolution filter to remove the effects of the seismic wavelet based on the optimization of the sparsity of the deconvolved reflectivity series. Several sparsity measures can be considered to this end. In this paper, we propose a simple modification of the hybrid l_1/l_2-norm loss function that enables it to be used as an unsupervised criterion for blind deconvolution (Takahata et al., 2012). In terms of computational complexity, the major advantage of MED algorithms is that the deconvolution filter can be obtained using only a small part of the section to be deconvolved; this filter is then used to deconvolve the whole section.

Finally, we note that in our approach, the deconvolution itself is performed by a linear filter; what we propose here is a method to design this filter. In contrast, SMBD and other multichannel approaches seek to directly determine the reflectivity (Rietsch, 1997a, 1997b; Kaaresen and Taxt, 1998; Kazemi and Sacchi, 2014). As we will see, this difference also helps to explain the reduced computational complexity of our approach. In terms of results, we will see that each approach has advantages and disadvantages.

THE CONVOLUTIONAL MODEL

In seismic data, the recorded traces are usually modeled by the convolution model as shown in Figure 1. The seismic data recorded at the jth receiver are given by

$$x_j(n) = s_j(n) * h(n) + \nu_j(n), j = 1, \ldots, J, \qquad (1)$$

where n refers to the temporal samples; $s_j(n)$ corresponds to the reflectivity series in the jth trace; $h(n)$ is the seismic wavelet, assumed to be the same for all traces; $\nu_j(n)$ is the additive noise; and J is the number of receivers. In the sequel, we will show how the assumption that all traces are affected by the same wavelet can be exploited to determine the reflectivities, even when the wavelet is unknown.

SPARSE MULTICHANNEL BLIND DECONVOLUTION

In this section, we review the blind multichannel method proposed by Kazemi and Sacchi (2014) to estimate the reflectivity series $s_j(n)$. To that end, consider the z-transform of the multichannel noiseless seismic data in equation 1, given by the following equation:

$$X_j(z) = H(z)S_j(z). \qquad (2)$$

By isolating the seismic wavelet $H(z)$, it can be shown (Kazemi and Sacchi, 2014) that

$$X_p(z)S_q(z) - X_q(z)S_p(z) = 0, \quad \forall\ p, q. \qquad (3)$$

In matrix notation, equation 3 can be expressed as

$$\mathbf{X}_p\mathbf{s}_q - \mathbf{X}_q\mathbf{s}_p = \mathbf{0}, \qquad (4)$$

where $\mathbf{X}_j$ represents the convolution matrix of the jth channel and $\mathbf{s}_j = [s_j(1), \ldots, s_j(N)]^T$. The combination of all possible equations, for all possible combinations of p and q, leads us to the following system of linear equations:

$$\mathbb{X}\mathbf{s} = \mathbf{0}, \qquad (5)$$

where

$$\mathbb{X} = \begin{bmatrix} \mathbf{X}_2 & -\mathbf{X}_1 & & & \\ \mathbf{X}_3 & & -\mathbf{X}_1 & & \\ \mathbf{X}_4 & & & -\mathbf{X}_1 & \\ \vdots & & & & \ddots \\ & \mathbf{X}_3 & -\mathbf{X}_2 & & \\ & \mathbf{X}_4 & & -\mathbf{X}_2 & \\ & \mathbf{X}_5 & & & -\mathbf{X}_2 \\ & \vdots & & & & \ddots \end{bmatrix}, \qquad (6)$$

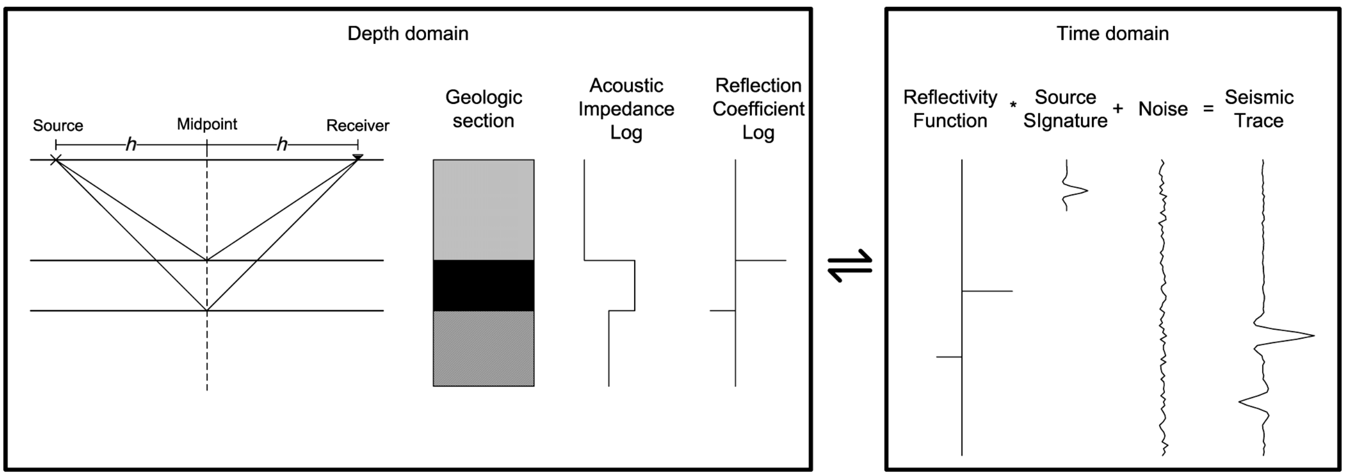

Figure 1. The convolution model in the depth and time domains.

and

$$\mathbf{s} = [\mathbf{s}_1^T, \mathbf{s}_2^T, \ldots, \mathbf{s}_J^T]^T. \quad (7)$$

In the noisy case, the linear system of equations becomes

$$\mathbb{X}\mathbf{s} = \mathbf{e}, \quad (8)$$

where $\mathbf{e}$ denotes the representation error, modeled as an additive noise term, which is not necessarily white and Gaussian (Kazemi and Sacchi, 2014).

In Kazemi and Sacchi (2014), the authors use a Bayesian approach (Kormylo and Mendel, 1983; Cheng et al., 1996; Rosec et al., 2003; Repetti et al., 2015) to estimate the reflectivity. Bayesian estimation usually aims at estimating the parameters $\mathbf{s}$ of a statistical model by solving the following problem:

$$\hat{\mathbf{s}} = \arg\min_{\mathbf{s}} f(\mathbb{X}, \mathbf{s}) + \lambda g(\mathbf{s}). \quad (9)$$

The function $f(\mathbb{X}, \mathbf{s})$ measures the fitness of the statistical model, whereas the regularization term $g(\mathbf{s})$ measures the fitness of a prior assumption about the parameters $\mathbf{s}$. For the problem at hand, Kazemi and Sacchi (2014) assume that the representation error $\mathbf{e}$ is white and Gaussian, so that $f(\mathbb{X}, \mathbf{s})$ can be written in terms of the log likelihood of a Gaussian random variable, which leads to the well-known mean-squared error. As prior information, they assume that the reflectivities are sparse, containing few nonzero values, and they use the hybrid l_1/l_2-norm function, also known as the pseudo-Huber function (Hartley and Zisserman, 2003; Huber and Ronchetti, 2009), as a sparsity-promoting regularization term. The resulting Bayes estimator is given by

$$\hat{\mathbf{s}} = \arg\min_{\mathbf{s}} \frac{1}{2}\|\mathbb{X}\mathbf{s}\|_2^2 + \lambda \sum_j \mathcal{R}_\epsilon(\mathbf{s}_j), \quad \text{subject to } \mathbf{s}^T\mathbf{s} = 1, \quad (10)$$

where

$$\mathcal{R}_\epsilon(\mathbf{s}_j) = \sum_n \left(\sqrt{s_j^2(n) + \epsilon^2} - \epsilon \right) \quad (11)$$

is the hybrid l_1/l_2-norm function. The constraint $\mathbf{s}^T\mathbf{s} = 1$ is imposed to avoid the trivial solution.

In robust statistics, the hybrid l_1/l_2-norm function is usually used when the data have outliers, i.e., large elements that would be unlikely under a Gaussian assumption. To better fit the data in this case, the assumed statistical distribution should have a heavier tail than that of the Gaussian. The hybrid l_1/l_2-norm function achieves this end automatically. In fact, if one thinks of the loss function as the log likelihood of a random variable, the corresponding distribution has a peak similar to the Gaussian distribution, but a tail resembles the Laplace distribution (Huber and Ronchetti, 2009; Repetti et al., 2015).

The hybrid l_1/l_2-norm function can also be seen as a smoothed version of the l_1 norm (Bube and Langan, 1997; Li et al., 2010; Zhang and Claerbout, 2011; Repetti et al., 2015), and hence it can be used as a measure of sparsity of a signal (Donoho, 2006). To illustrate such a relationship, consider the function,

$$z_j(n) = \sqrt{y_j^2(n) + \epsilon^2} - \epsilon. \quad (12)$$

In Figure 2a and 2b, we plot this function, along with $y_j(n)$, related to the l_1 norm. From this figure, it is possible to observe that the hybrid l_1/l_2-norm function resembles the l_2 norm for $y_j \ll \epsilon$ and to the l_1 norm for $y_j \gg \epsilon$.

The ability of the hybrid l_1/l_2-norm function to measure the sparsity of a signal has already been exploited in seismic deconvolution (Zhang and Claerbout, 2011). In the next section, we propose to use this function to perform multichannel deconvolution based on an MED framework.

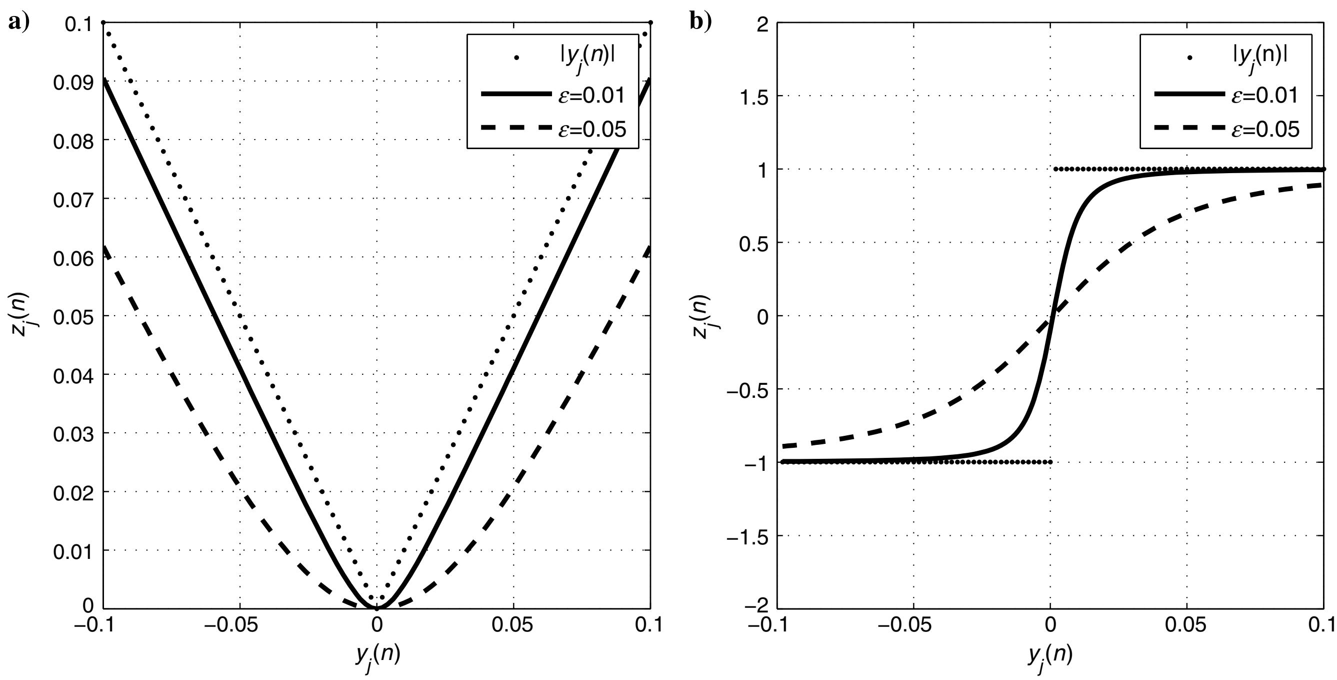

Figure 2. (a) Comparison of the absolute value and its approximation with the function $z_j(n)$ for different values of ϵ, followed by its respective first-order derivative (b).

A FAST ALGORITHM FOR SPARSE MULTICHANNEL BLIND DECONVOLUTION

The deconvolution method reviewed in the previous section requires the solution of the optimization problem in equation 10, which can be costly. However, the solution of equation 10 yields the reflectivity functions, gathered in the vector **s**. An alternative, simpler approach is to use the Bayesian framework to seek good deconvolution filters. Once these linear filters are designed, they can be applied to the seismic data $x_j(n)$ to determine the reflectivities.

In the context of this paper, the minimum entropy criterion for filter design is a very interesting approach. MED has been first introduced by Wiggins (1978). It is based on the prior assumption that the convolution of the reflectivity series, which is sparse, with the seismic wavelet will produce a less sparse signal. Hence, deconvolution can be achieved with a deconvolution filter able to retrieve the most sparse signal, which corresponds to the original signal. Sufficient and necessary conditions for that can be found in Donoho (1981), Shalvi and Weinstein (1990), Nose-Filho et al. (2014), and Nose-Filho and Romano (2014).

In this case, the solution does not depend on the magnitude of the filter coefficients, nor on its intrinsic delay (Shalvi and Weinstein, 1990). Hence, the adaptation/optimization of the filter coefficients can be done by means of the optimization of an invariant scale function able to measure the degree of sparsity of a given signal (Hurley and Rickard, 2009). As a consequence, local minima are to be expected and may correspond to the set of desirable solutions, i.e., to delayed and scaled versions of the inverse filter.

For the adaptation/optimization of the filter coefficients, several different measures could be used. If one defines a sparse signal as being a signal composed of a few spikes separated by exactly zero terms, one may prefer l_0 or l_1 norm. However, if one refers to a sparse signal as a signal composed of a few spikes separated by nearly zero terms, then, one may prefer to use smoother functions, such as the varimax norm (Wiggins, 1978), the smooth l_0 norm (Nose-Filho et al., 2014), or any other norm, different from the l_0 and the l_1 norms (Gray, 1978a, 1978b; Ooe and Ulrych, 1979; Donoho, 1981; Cabrelli, 1985; Nandi et al., 1997; Nose-Filho and Romano, 2014).

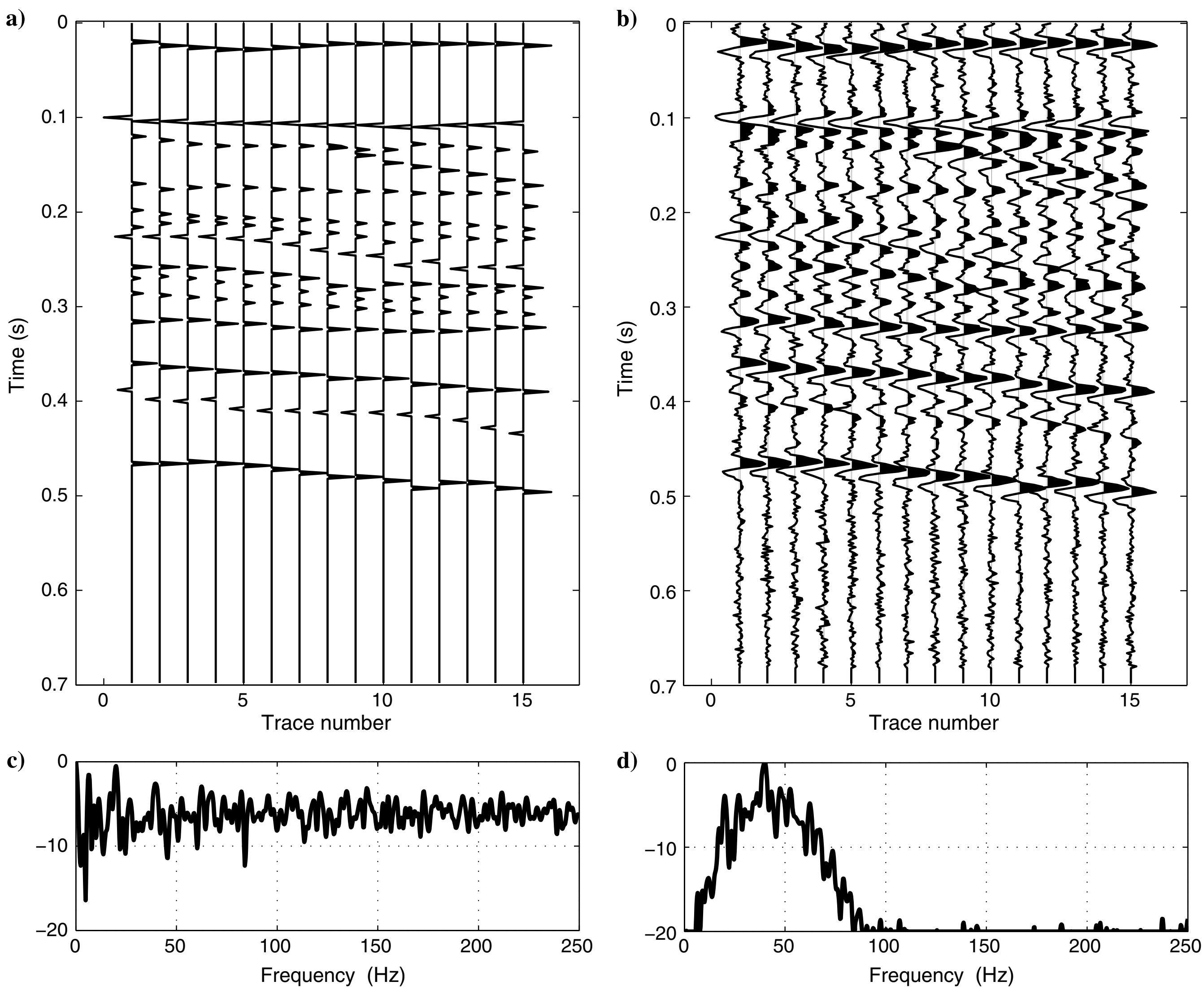

Figure 3. (a) Original reflectivity series and (b) synthetic seismogram with 9 dB of S/N, followed by its respective power spectral density (c and d).

In this paper, we propose the use of the hybrid l_1/l_2-norm function to obtain the coefficients of the deconvolution filter. This preference relies on the fact that it is a smooth function, so that simple gradient-based methods can be used in the optimization. However, as stated before, an appropriate criterion for any unsupervised technique must be scale invariant, which is not the case of the hybrid l_1/l_2-norm function. Thus, we propose to normalize it by the variance of the deconvolved signal. To express this new criterion, let $y_j(n)$ be the deconvolved traces, obtained as the output of a deconvolution filter with impulse response $w(n)$:

$$y_j(n) = x_j(n) * w(n) = \sum_k w(k) x_j(n-k). \qquad (13)$$

The normalized cost function is then given by

$$\mathcal{R}_\epsilon(\mathbf{y}_j) = \sum_n \left(\sqrt{\frac{y_j^2(n)}{\sigma_{\mathbf{y}_j}^2} + \epsilon^2} - \epsilon \right), \qquad (14)$$

where $\sigma_{\mathbf{y}_j}^2 = \sum_n y_j^2(n)/N$ is the estimated variance of the estimated reflectivity series.

In a multichannel framework, the MED filter is the solution of the following optimization problem:

$$\hat{\mathbf{w}} = \underset{\mathbf{w}}{\operatorname{argmin}} \; J(\mathbf{y}) = \sum_j \mathcal{R}_\epsilon(\mathbf{y}_j),$$
$$\text{subject to } \mathbf{w}^T\mathbf{w} = 1, \qquad (15)$$

where the constraint $\mathbf{w}^T\mathbf{w} = 1$ is provided to avoid the trivial solution.

The optimization of the coefficients of the deconvolution filter is performed by means of a simple gradient-descent algorithm. The derivative of the normalized hybrid l_1/l_2-norm function with respect to the kth coefficient of the filter $\mathbf{w}$ is given by

$$\frac{\partial J(\mathbf{y})}{\partial w_k} = \sum_j \sum_n \frac{(z_j(n))^{-1/2}}{\sigma_{\mathbf{y}_j}^2} \left(y_j(n) x_j(n-k) - \frac{y_j(n)^2}{N} \sum_n y_j(n) x_j(n-k) \right), \qquad (16)$$

where we redefine $z_j(n)$ as $z_j(n) = y_j^2(n)/\sigma_{\mathbf{y}_j}^2 + \epsilon^2$.

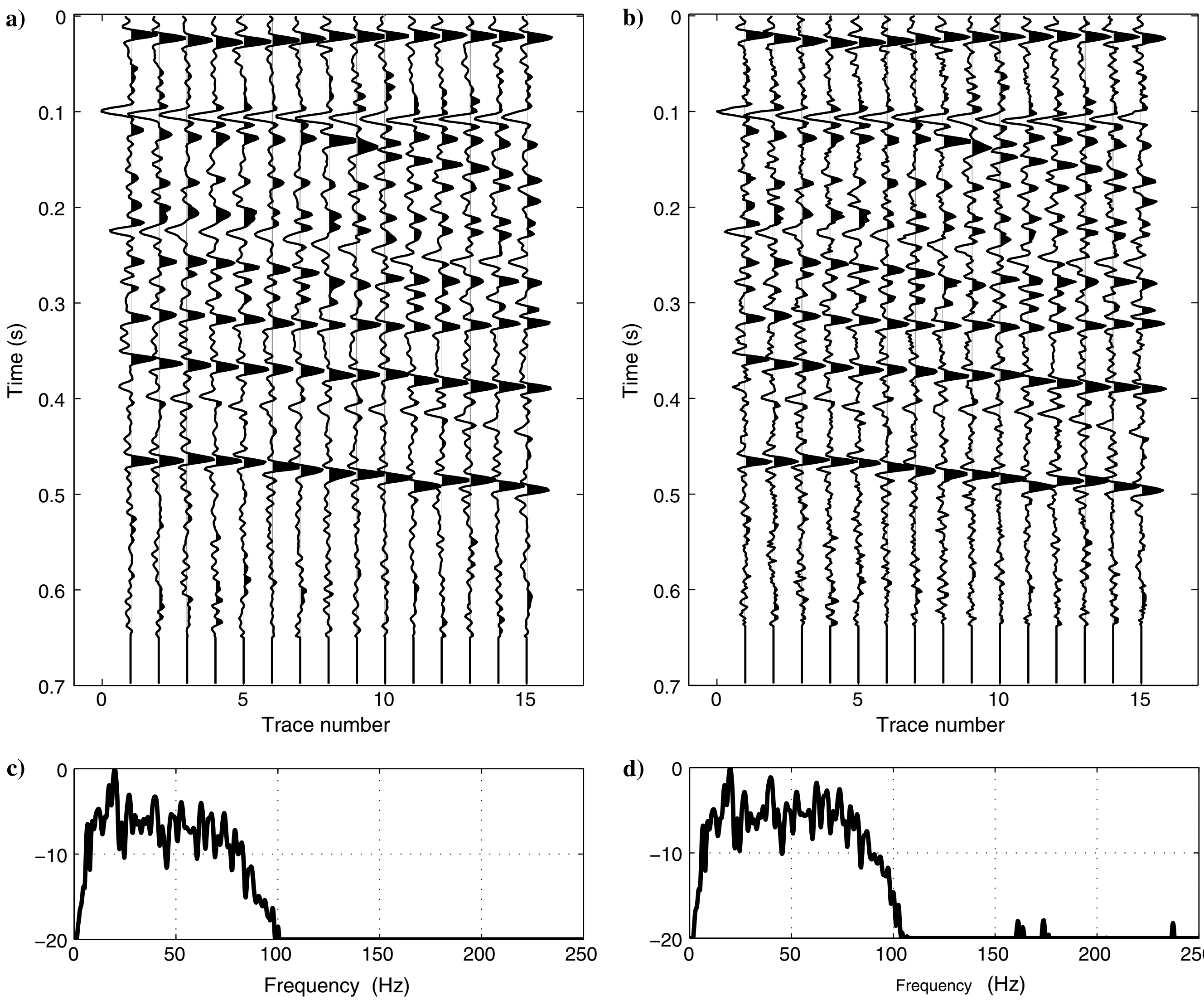

Figure 4. Deconvolved section with (a) F-SMBD and (b) LS, followed by its respective power spectral density (c and d).

Thus, the adaptation of $\mathbf{w}$ is given by

$$\mathbf{w}(m+1) = \mathbf{w}(m) - \mu \nabla J(\mathbf{w}(m)),$$
$$\mathbf{w}(m+1) = \frac{\mathbf{w}(m+1)}{\|\mathbf{w}(m+1)\|_2^2}, \quad (17)$$

where μ is the step size of the gradient algorithm. The second step in equation 15 ensures that the constraint $\mathbf{w}^T\mathbf{w} = 1$ is met at every iteration (Douglas et al., 2000).

It is worth mentioning that the optimization problem in equation 15 may present some local minima, so that the gradient descent algorithm must be carefully initialized. A good initialization can be made by a single spike of unit magnitude located according to some previous assumption on the phase of the wavelet (Shalvi and Weinstein, 1990). For example, for minimum-phase wavelets, it is advisable to initialize the deconvolution filter with a single spike at the beginning of the filter. For mixed-phase wavelets, it is advisable to initialize it with a single spike located at the middle of the filter, and in the case of maximum-phase wavelets, it is advisable to initialize it with a spike at the end.

For simplicity, from now on, the method proposed by Kazemi and Sacchi (2014) will be referred to as SMBD, whereas the method that we propose will be referred to as fast SMBD (F-SMBD).

A detailed analysis of the computational cost of each algorithm is a difficult task, and it is outside the scope of this work. However, to give a general idea of the reduction in computational cost achieved by our proposal, we will compare the size of matrix $\mathbb{X}$ in equation 10, which refers to SMBD, and the size of the convolution matrix for computing the output of the deconvolution filter, which refers to F-SMBD. The SMBD is extremely costly because it compares all channels with all channels, leading to a matrix of dimension $((J(J-1)(N+L-1))/2 \times JN)$, where J is the number of channels, N is the number of samples, and L is the length of the wavelet. However, the proposed algorithm makes use only of the multichannel convolution matrix of dimension $((N+L-1) \times JN)$, i.e., $(J(J-1))/2$ times smaller than $\mathbb{X}$.

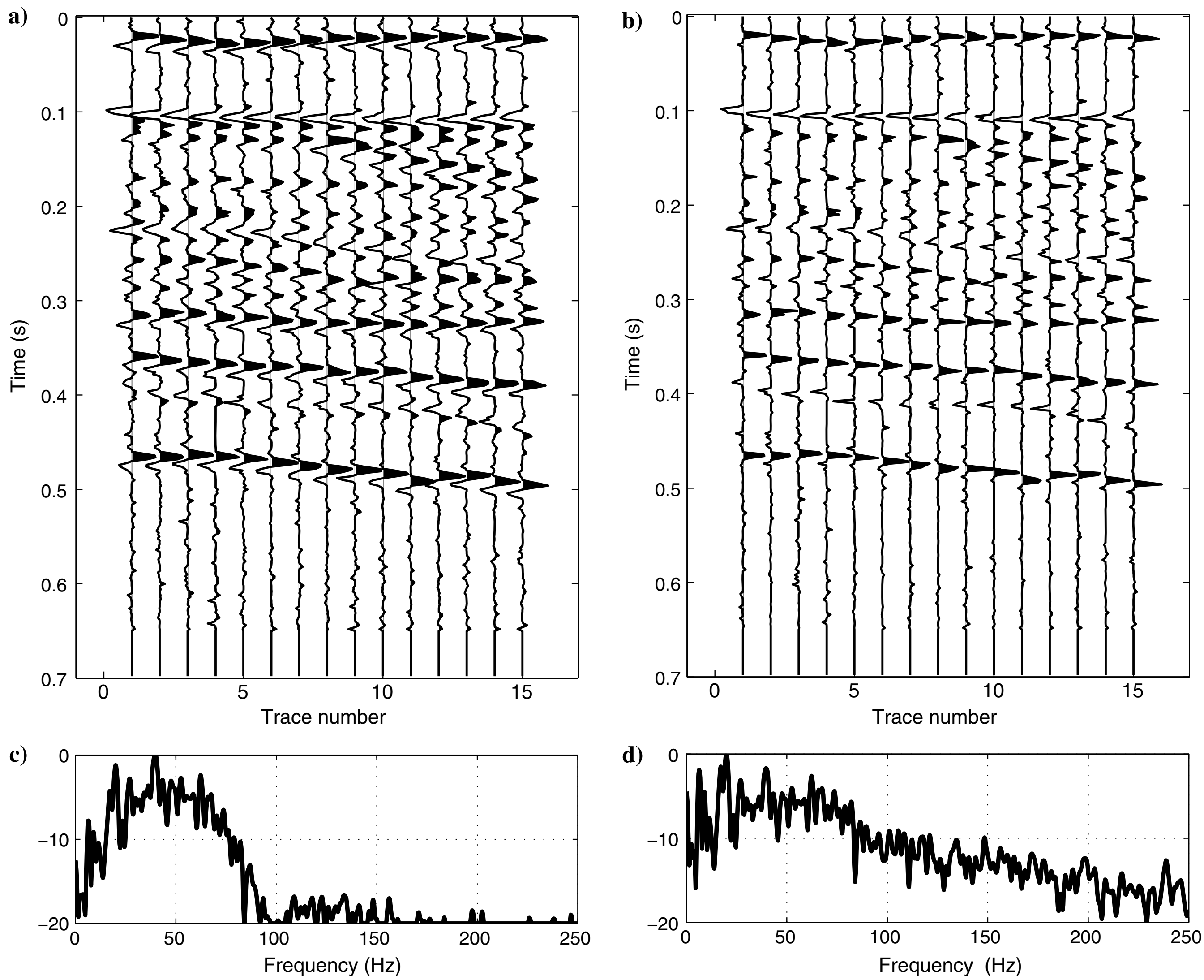

Figure 5. Deconvolved section with SMBD for different values of λ: (a) $\lambda = 5$ and (b) $\lambda = 10$, followed by its respective power spectral density (c and d).

In the following, we present some results illustrating the performance of both algorithms with synthetic and real data.

RESULTS

In this section, we illustrate results obtained for both algorithms with synthetic and real data. As a figure of merit for the estimated reflectivity, we will use the Pearson correlation coefficient (Gibbons and Chakraborti, 2010), given by

$$r = \frac{\mathbf{s}^T \mathbf{y}}{\|\mathbf{s}\|_2 \|\mathbf{y}\|_2}, \tag{18}$$

where $\mathbf{s}$ corresponds to the true reflectivity and $\mathbf{y}$ corresponds to its estimate. Note that the output of the deconvolution filter may have an unknown delay with respect to the actual reflectivity $\mathbf{s}$ (Ding and Li, 2001). To fix this, we compute the correlation coefficient for several delayed versions of the filter output; the estimated reflectivity $\mathbf{y}$ corresponds to the delay that yields the largest r. In other words, $\mathbf{y}$ is the delayed filter output that best aligns with the actual reflectivity $\mathbf{s}$.

Synthetic results

First, we test the proposed method in a synthetic example with additive white Gaussian noise with a signal-to-noise ratio (S/N) of 9 dB. The true reflectivity is shown in Figure 3a, and the synthetic data are shown in Figure 3b. In this example, we use a Ricker wavelet with a central frequency of 40 Hz and a 5° phase rotation. To benchmark our results, we also use an ideal least-squares (LS) deconvolution filter, designed under the assumption that the reflectivity series is known.

For the F-SMBD algorithm, we use a deconvolution filter of length 51, initialized with a single spike located at the middle of the filter, $\epsilon = 1$, a learning rate of $\mu = 0.02$, and 1000 iterations as the stop criterion. In the SMBD method, there are two parameters to be adjusted: the regularization parameter and the hybrid norm parameter (ϵ). Moreover, the second one just needs to be a very small number to approximate the l_1-norm behavior. The SMBD algorithm is run for two different values of λ (recall that λ is the parameter that controls the weight of the regularization term in SMBD [refer to equation 10]; in this case, two different values are used to obtain a less sparse reflectivity $[\lambda = 5]$ and a sparser reflectivity $[\lambda = 10]$), $\lambda = 5$ and $\lambda = 10$, we assume that the wavelet length is approximately 5 ms, $\epsilon = 0.0005$, a maximum of five iterations for each line search and 200 iterations as the stop criterion. It is worth mentioning that the difference between parameter ϵ used in the algorithms is due to the use of the proposed normalized version of the hybrid l_1/l_2-norm criterion in the F-SMBD.

The results obtained with the F-SMBD and the LS algorithm are presented in Figure 4a and 4b, respectively. All of them are followed by their respective power spectral densities. The results obtained for the SMBD algorithm for the different values of λ are presented in Figure 5a and 5b. As one can see, the results of SMBD are full band, meanwhile the results of F-SMBD are band-limited. To have a fair comparison, we apply a band-pass filter in the results of SMBD with corner frequencies of 1, 10, 100, and 125 Hz before calculating its Pearson correlation coefficient with respect to the actual reflectivity. The Pearson correlation coefficients are as follows: 0.45 for the synthetic data, 0.52 for the F-SMBD, 0.56 for the ideal LS filter, and 0.51 and 0.60 for the two values of λ in the SMBD. These results illustrate that the proposed algorithm almost reaches the best performance possible for a filtering approach, which is obtained by the supervised LS filter. Despite the fact that SMBD presents a more spikelike deconvolution, it is worth observing that, from the deconvolved section with F-SMBD, it is possible to retrieve the true reflectors by comparing Figures 3a and 4a. In addition, we can add the

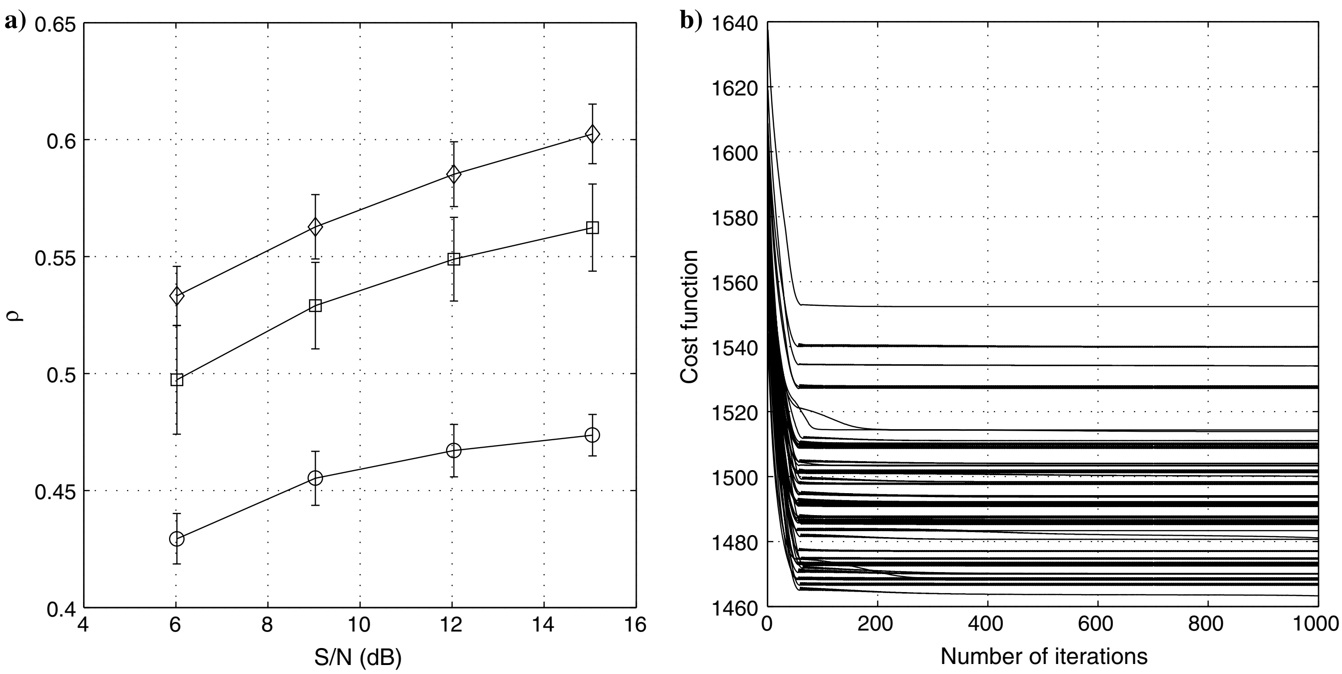

Figure 6. (a) Mean and standard deviation of the Pearson correlation coefficient for (diamonds) LS filter, (squares) F-SMBD, and (circles) the synthetic data with the original reflectivity and (b) converge curves (cost function × number of iterations) for each Monte-Carlo simulation for the 9-dB S/N case.

facts that SMBD may not preserve some amplitudes' relations and it may kill some events. In the case of F-SMBD, this is also true, but the use of a single linear operator may cause only linear distortions, and it is more aligned with most of the methods that are used in seismic deconvolution.

To analyze the stability of the proposed algorithm, we ran a Monte Carlo simulation with 50 different realizations of noise and reflectivity for different S/Ns. The reflectivity series is generated by a Bernoulli Gaussian random variable with the probability of having a nonzero value equal to 0.1. However, due to the fact that

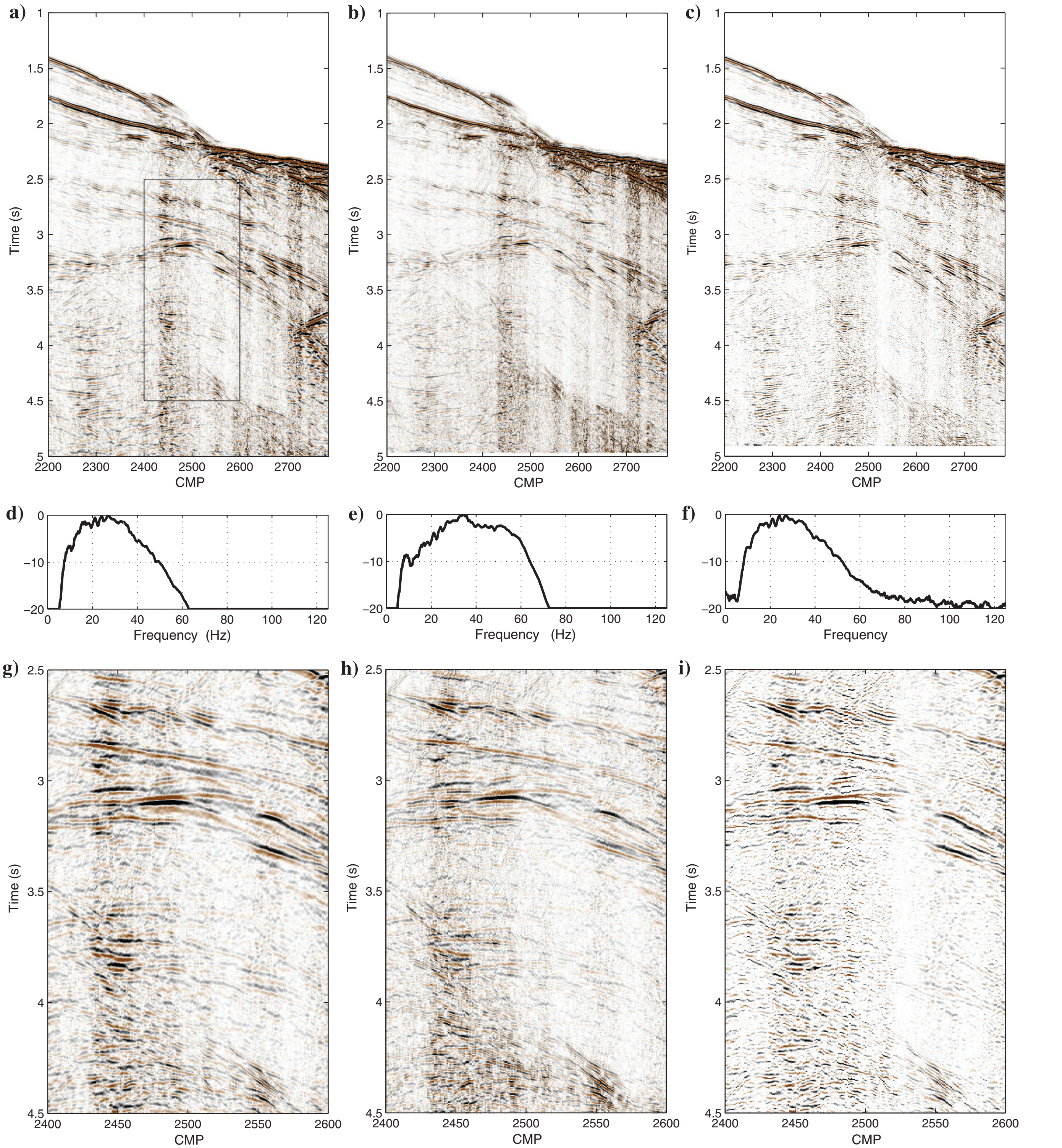

Figure 7. (a) The stacked section and its deconvolution with (b) F-SMBD and (c) SMBD, followed by its respective power spectral density (d-f) and magnification (g-i) performed in the black rectangle illustrated in panel (a).

the Pearson correlation coefficients are bounded, they are not normally distributed. Thus, for the calculation of its mean and standard deviation, a transformation is necessary to have an unbiased estimation. In this case, we make use the Fisher's z-transform (Silver and Dunlap, 1987; Kazemi and Sacchi, 2014), given by the following equation:

$$z = \frac{1}{2} \ln\left(\frac{1+r}{1-r}\right). \tag{19}$$

The statistics are calculated over the z-transformed coefficients and transformed back to the Pearson correlation coefficients by means of the following transformation:

$$r = \frac{\exp(2z) - 1}{\exp(2z) + 1}. \tag{20}$$

The mean and standard deviation of the Pearson correlation coefficient for these experiments are illustrated in Figure 6a, in which we also show the results obtained with the LS filter. From this figure, it is possible to observe that the proposed algorithm produces results that are quite close to the one obtained with the supervised approach, with small standard deviation, indicating the stability of F-SMBD. To illustrate the convergence of F-SMBD, we also provide the convergence curves (cost function × number of iterations) for each Monte-Carlo simulations for the 9-dB S/N case, illustrated by the curves of Figure 6b.

Real data results

In this subsection, we present some results obtained with F-SMBD and the SMBD algorithm for real marine seismic data. These stacked data are shown in Figure 7a.

The parameters for the F-SMBD algorithm were a deconvolution filter with 21 coefficients, initialized with a single spike at the middle of the filter; a learning rate of $\mu = 0.1$, $\epsilon = 1$; and 1000 iterations as a stop criterion. The deconvolution filter was designed using only one part of the data, comprising the common midpoint 2239–2241 from 1.3960 to 1.9960 s (which comprises three traces of the first break).

The parameters for the SMBD algorithm were $\lambda = 5$, a wavelet length of 10 ms, $\epsilon = 0.0001$, a maximum of five iterations for each line search and 200 iterations as the stop criterion. In this case, we used a spatial window with 25 traces and 20% overlapping.

In Figure 7b and 7c, we illustrate the results obtained for both algorithms and the resulting power spectral densities. In spite of the fact that SMBD provides a more spikelike deconvolution, F-SMBD offers improvements to the vertical resolution in terms of much less time used and with much lower computational cost. In terms of power spectral densities, the proposed algorithm is able to provide a more significant gain in the frequency range of 40–60 Hz. In terms of the computational cost, although SMBD took almost 1 h to provide the results, the proposed algorithm took just a few seconds.

CONCLUSIONS

In this paper, we address blind deconvolution in a multichannel framework by means of an MED algorithm. MED seeks to determine a deconvolution filter able to retrieve, in its output, the most sparse signals. As such, it is expected that the deconvolved signal should resemble the reflectivity series. Our proposal relies on a modification of the hybrid l_1/l_2-norm function to make it scale invariant and, hence, suitable for being used as an unsupervised criterion. For the optimization of the coefficients of the deconvolution filter, we used a simple gradient-based algorithm.

One of the main advantages of the MED algorithm is that it can be used in a multichannel framework with very low computational cost. This is because the deconvolution filter can be optimized using a small part of the seismic section, and once the filter is optimized, it can be used to deconvolve the whole section.

We compare our method with an SMBD algorithm, which also uses the hybrid l_1/l_2-norm function, but in a Bayesian estimation framework. Despite the very good results obtained with such an algorithm, it is computationally costly because it requires the comparison of all channels with all channels. In fact, its cost grows quadratically with the number of channels.

In our results, for the synthetic and real data scenarios, one may see a trade-off between spikiness and computational cost. Although SMBD provides a more spikelike deconvolution, F-SMBD improves quite well the vertical resolution with much less computational cost.

ACKNOWLEDGMENTS

K. Nose-Filho would like to thank CAPES and CNPq for funding his doctoral research. The authors would like to thank Petrobras for the financial support.

REFERENCES

Bube, K. P., and R. T. Langan, 1997, Hybrid l_1/l_2 minimization with applications to tomography: Geophysics, **62**, 1183–1195, doi: 10.1190/1.1444219.
Cabrelli, C. A., 1985, Minimum entropy deconvolution and simplicity: A noniterative algorithm: Geophysics, **50**, 394–413, doi: 10.1190/1.1441919.
Cheng, Q., R. Chen, and T. H. Li, 1996, Simultaneous wavelet estimation and deconvolution of reflection seismic signals: IEEE Transactions on Geoscience and Remote Sensing, **34**, 377–384, doi: 10.1109/36.485115.
Claerbout, J. F., 1977, Parsimonious deconvolution: Stanford Exploration Project, Technical report 13.
Ding, Z., and Y. Li, 2001, Blind equalization and identification: Marcel Dekker.
Donoho, D. L., 1981, On minimum entropy deconvolution: Academic Press.
Donoho, D. L., 2006, For most large undetermined systems of equations, the minimal l-norm near-solution approximates the sparsest near-solution: Communications on Pure and Applied Mathematics, **59**, 907–934, doi: 10.1002/cpa.20131.
Douglas, S. C., S. I. Amari, and S. Y. Kung, 2000, On gradient adaptation with unit-norm constraints: IEEE Transactions on Signal Processing, **48**, 1843–1847, doi: 10.1109/78.845952.
Gibbons, J. D., and S. Chakraborti, 2010, Nonparametric statistical inference: Chapman and Hall/CRC.
Gray, W., 1978a, A theory for variable norm deconvolution: Stanford Exploration Project, Technical report 15.
Gray, W., 1978b, Variable norm deconvolution: Stanford Exploration Project, Technical report 14.
Hartley, R., and A. Zisserman, 2003, Multiple view in geometry computer vision: Cambridge University Press.
Huber, P. J., and E. M. Ronchetti, 2009, Robust statistics, 2nd ed.: Wiley.
Hurley, N., and S. Rickard, 2009, Comparing measures of sparsity: IEEE Transactions on Information Theory, **55**, 4723–4741, doi: 10.1109/TIT.2009.2027527.
Inouye, Y., and T. Sato, 1996, Unconstrained optimization criteria for blind equalization of multichannel linear systems of nonminimum phase, *in* Proceedings of the 1996 International Conference on Signal Processing 1, IEEE, 416–419.
Kaaresen, K. F., and T. Taxt, 1998, Multichannel blind deconvolution of seismic signals: Geophysics, **63**, 2093–2107, doi: 10.1190/1.1444503.
Kazemi, N., and M. D. Sacchi, 2014, Sparse multichannel blind deconvolution: Geophysics, **79**, no. 5, V143–V152, doi: 10.1190/geo2013-0465.1.
Kormylo, J. J., and J. M. Mendel, 1983, Maximum-likelihood seismic deconvolution: IEEE Transactions on Geoscience and Remote Sensing, **GE-21**, 72–82, doi: 10.1109/TGRS.1983.350532.
Kundur, D., and D. Hatzinakos, 1996, Blind image deconvolution: Signal Processing Magazine, **13**, no. 3, 43–64, doi: 10.1109/79.489268.

Li, Y., Y. Zhang, and J. Claerbout, 2010, Geophysical applications of a novel and robust L1 solver: 80th Annual International Meeting, SEG, Expanded Abstracts, 3519–3523.

Misra, S., and S. Chopra, 2011, Mixed-phase wavelet estimation — A case study: CSEG Recorder, **36**, 32–35.

Nandi, A. K., D. Mampel, and B. Roscher, 1997, Blind deconvolution of ultrasonic signal in nondestructive testing applications: IEEE Transactions on Signal Processing, **45**, 1382–1390, doi: 10.1109/78.575716.

Nose-Filho, K., C. Jutten, and J. M. T. Romano, 2014, Sparse blind deconvolution based on scale invariant smoothed ℓ_p-norm: Presented at 22nd European Signal Processing Conference.

Nose-Filho, K., and J. M. T. Romano, 2014, On ℓ_p-norm sparse blind deconvolution: Presented at IEEE International Workshop on Machine Learning for Signal Processing, doi: 10.1109/MLSP.2014.6958864.

Ooe, M., and T. J. Ulrych, 1979, Minimum entropy deconvolution with an exponential transformation: Geophysical Prospecting, **27**, 458–473, doi: 10.1111/j.1365-2478.1979.tb00979.x.

Porsani, M. J., and B. Ursin, 1998, Mixed phase deconvolution: Geophysics, **63**, 637–647, doi: 10.1190/1.1444363.

Proakis, J. G., 2001, Intersymbol interference in digital communication systems: Wiley Online Library.

Ram, I., I. Cohen, and S. Raz, 2010, Multichannel deconvolution of seismic signals using statistical MCMC methods: IEEE Transactions on Signal Processing, **58**, 2757–2770, doi: 10.1109/TSP.2010.2042485.

Repetti, A., M. Q. Pham, L. Duval, E. Chouzenoux, and J.-C. Pesquet, 2015, Euclid in a taxicab: Sparse blind deconvolution with smoothed l_1/l_2 regularization: IEEE Signal Processing Letters, **22**, 539–543, doi: 10.1109/LSP.2014.2362861.

Rietsch, E., 1997a, Euclid and the art of wavelet estimation, Part I: Basic algorithm for noise-free data: Geophysics, **62**, 1931–1938, doi: 10.1190/1.1444293.

Rietsch, E., 1997b, Euclid and the art of wavelet estimation, Part II: Robust algorithm and field-data examples: Geophysics, **62**, 1939–1946, doi: 10.1190/1.1444294.

Robinson, E. A., 1954, Predictive decomposition of time series with applications to seismic exploration: Ph.D. thesis, Massachusetts Institute of Technology.

Romano, J. M. T., R. Attux, C. C. Cavalcante, and R. Suyama, 2011, Unsupervised signal processing: Channel equalization and source separation: CRC Press.

Rosec, O., M. Boucher, B. Nsiri, and T. Chonavel, 2003, Blind marine seismic deconvolution using statistical MCMC methods: IEEE Journal of Oceanic Engineering, **28**, 502–512, doi: 10.1109/JOE.2003.816683.

Shalvi, O., and E. Weinstein, 1990, New criteria for blind deconvolution of nonminimum phase systems (channels): IEEE Transactions on Information Theory, **36**, 312–321, doi: 10.1109/18.52478.

Silver, N. C., and W. P. Dunlap, 1987, Averaging correlation coefficients: Should Fisher's z transformation be used?: Journal of Applied Psychology, **72**, 146–148, doi: 10.1037/0021-9010.72.1.146.

Takahata, A. K., E. Z. Nadalin, R. Ferrari, L. T. Duarte, R. Suyama, R. R. Lopes, J. M. T. Romano, and M. Tygel, 2012, Unsupervised processing of geophysical signals: IEEE Signal Processing Magazine, **29**, no. 4, 27–35, doi: 10.1109/MSP.2012.2189999.

Wiggins, R. A., 1978, Minimum entropy deconvolution: Geoexploration, **16**, 21–35, doi: 10.1016/0016-7142(78)90005-4.

Xu, G., H. Liu, L. Tong, and T. Kailath, 1995, A least-squares approach to blind channel identification: IEEE Transactions on Signal Processing, **43**, 2982–2993, doi: 10.1109/78.476442.

Yilmaz, O., 2001, Seismic data analysis: Processing, inversion and interpretation of seismic data: SEG.

Zhang, Y., and J. Claerbout, 2011, A new bidirectional deconvolution method that overcomes the minimum phase assumption: Stanford Exploration Project, Technical report 142.